On focusing properties of graded index photonic crystals

A. GHARAATI[*], N. MIRI
Physics Department, Payame Noor University, Tehran, Iran

In this paper, we have studied the focusing behavior of two-dimensional Graded Index (GRIN) Photonic Crystal (PC). Two different structures have been considered which were labeled as the structure type I and the structure type II. To create an index gradient, the rods (holes) radii have been varied along the direction transverse to the propagation. Several optical phenomena such as focusing, de-focusing, and collimation have been investigated regarding structure type I. Also, the focusing effect has been analyzed for the GRIN PC structure type I and type II. In addition, detailed investigations were carried out by comparing the focusing characteristics of two structures. The obtained results have illustrated that the GRIN PC type II represents stronger focusing characteristics in comparison to the GRIN PC type I. Furthermore, by increasing the structural length of both GRIN PCs while the normalized frequency of incoming wave is constant, the focal length decreases although the concentration intensity rises.

1. Introduction

Photonic crystals (PCs) are periodic structures in which the refractive index varies in one, two, or three directions. Two dimensional PCs stand as the periodic arrangement of high and low refractive index in two dimensions. Arising from the differences between refractive indices, we have the band structure that consists of allowed and forbidden bands. After the invention of photonic crystals by pioneering work of E. Yablonovitch and S. John [1, 2], in 1987, several special properties of PCs, such as super-prism [3, 4], self-collimation [5-7], self-guiding [8], routing [9], slow light [10] and negative-refraction [11] have been investigated. PCs with large photonic band gaps (PBG) are an appropriate choice for designing micro-cavities [12-14], couplers [15], waveguides [16-18], filters, and optical fibers [19]. Besides, the literature has reported the use of PCs in implementing various devices including laser [20], splitter [21-22], sensor [23], reflector, [24] and photon trapping /emitting structure [25]. The concept of GRIN PC, which has improved the ability of controlling light propagation direction, has been introduced by utilizing the modified PC. Various types of GRIN PC structures have been considered through the literatures [26-30]. A GRIN PC structure can be designed by employing the gradual modifications of lattice period, the filling factor or the refractive index of the material, which results in the generation of index gradients. GRIN PCs contain the potential for various applications such as wavelength de-multiplexer [31-32], effective mode coupler, [33] and mode order converter [34]. As the very first work, the GRIN PC was proposed by E. Centeno, in 2005, for light bending effects [35]. One year later, a GRIN PC that presented mirage and super-bending effects that could be used for designing a bent waveguide was proposed by the

same group [36]. A new methodology was discovered for designing GRIN PC structure that displayed self-collimation and focusing effects capable of realizing the focusing (lens) and guiding (waveguide) effects and thus, more complex optical devices such as couplers could have been designed [37]. A novel approach was proposed that for implementing GRIN PC structures has been described in which the lattice spacing has been altered along the transverse direction to propagation. In comparison to the traditional massive and bulky lenses, the designed GRIN PCs are capable of being utilized in optical systems that require compact and powerful focusing elements [38]. Moreover, the Mirage effect has been demonstrated by metallic graded photonic crystal [39]. Parabolic and triangular GRIN PCs was proposed to design beam aperture modifier and beam deflector [40-41]. It is suggested to bend the GRIN PC structure in order to achieve GRIN waveguide for the purpose of bending and guiding light with high efficiency in the desired direction [42]. It has been proposed in [43] a secant hyperbolic profile of effective refractive index in GRIN PC with varying lattice spacing in order to show focusing, diverging and collimation effect in both low and high frequency regimes. Although more details have been explored and discovered on dielectric GRIN PC [44]. Moreover, GRIN PCs with elliptical elements have been studied for various photonic applications such as focusing lenses [45-47], laser light production applications [48], and self-collimation mechanism [49-51]. Few studies have been devoted to PC structures with rectangular and diamond-shaped elements [52-53]. To control and enrich the polarization insensitive ability of light the annular GRIN PC was proposed [54]. Besides, an adaptive GRIN PC lens was designed by using liquid crystals [55]. Recently, the focusing effect of the GRIN PC structures with different refractive index of background material has

been investigated by means of the effective medium theory [56].

However, in this paper, we have enquired into the optical effects such as focusing, de-focusing, and collimation. Our work has brought more details about the dependency of focal point position on structural length and variation of FWHM with respect to the number of columns. Focusing characteristic has been put into comparison regarding two different structures. One of them was composed of dielectric rods in air background and the other structure was made of air holes in dielectric background, while they both contained square lattices. The Finite-Difference Time-Domain (FDTD) [57] method has been used to simulate the propagation of electromagnetic waves through the structure. Furthermore, the plane wave expansion (PWE) [58] has been utilized to calculate the band structure.

2. Modeling

Two PC structures have been considered as the following: structure type I which is made of dielectric rods in air background and structure type II that is made of air holes in dielectric background, while both of them are in square lattice. A GRIN PC has been designed by varying the rods radii in the direction transverse to propagation. A GRIN medium can be initiated by a PC, in which the rod's radii are changed while the refractive index of material and lattice spacing are kept intact. For a certain column, rod (hole) radii are altered in the direction transverse to the propagation. In structure type I, rod radii are varied from 0.10a to 0.45 by an increased stepwise 0.05a, while regarding structure type II, hole radii are varied from 0.10a to 0.45a with the same increased stepwise but in the opposite direction. The GRIN PCs geometry is presented in Fig. 1.

At first, the PWE method has been employed to calculate the dispersion diagram along Γ-X direction for the first band of PCs with different dielectric rod (air hole) radii. The results are illustrated in Fig 2(a) for structure type I and through Fig. 3(a) for structure type II. The increasing radius of rods, while the refractive index and lattice spacing are constant, results in the shift of related bands towards the lower frequencies. In contrast, when air hole radii increase, the related bands move towards higher frequencies. For a certain column, rods radius increases from 0.05a to 0.45a with step of 0.05a in which a stands as the lattice spacing. The value of rod radius increases from the edges to the center. The gradient of refractive index is present only in the transverse y-direction. To change the refractive index of dielectric rods, it is required to utilize different materials; therefore, the refractive index is kept equal to 2.
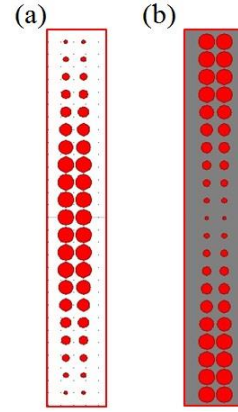

Fig. 1. The schematic representation of GRIN PC structures (a) type I and (b) type II, the lattice spacing is constant, but the radii are varied

As the second step, we calculate the group index from the slop information of each band involved in dispersion diagram, which can be done through the following relation:

$$N_g = c / \nabla_k \omega(k)$$

(1)

In which c stands as the light velocity in vacuum, ω would be the angular frequency, and k is the wave vector. The group index is referred to as the effective refractive index (n_{eff}). The result is demonstrated in Fig. 2(b), representing the effective refractive index as a function of normalized frequency for different values of rod radii regarding structure type I. Fig. 3(b) displays the n_{eff} as a function of normalized frequency (ωa/2πc) of structure type II. For longer wavelength or lower frequency, the effective index curves are closely spaced and thus, there exists a smooth variation in the effective index. Therefore, by getting closer to the edges (cut region), we can observe a nonlinear behavior of dispersion in the effective index curves. Each curve enters the cut region at a different frequency while strong dispersion can be noticed in these regions. As the last step, we intend to design a GRIN PC structure with a certain profile of refractive index in a fixed frequency. This frequency is selected from the region that contains smooth variation in effective index. The GRIN PC structure is designed at a normalized frequency equal to a/λ=0.18. In the fixed frequency of a/λ=0.18, effective index changes from 1.104 to 1.747. Now it is possible to calculate the effective index as a function of rod radius when the frequency is fixed. Fig. 2(c) exhibits the effective refractive index as a function of rod radius variation for the structure type I and Fig. 3(c) shows the effective refractive index as a function of air hole radius for the structure type II. To obtain a GRIN PC structure with any desired profile of refractive index distribution in the range of 1.457 to 1.970, it is required to procure the intermediate point of refractive index that provides a smooth variation in the effective index. For this reason, interpolation method has been applied to

obtain the intermediate point by fitting the effective refractive index profile of square cells with different radii of dielectric rod, which varies from 0.10a to 0.45a. Then, the desired GRIN PC structure was constructed by gradually changing the rod (hole) radius and having those intermediate n_{eff} values remaining in such a way that the concerning index distribution would become perceptible.
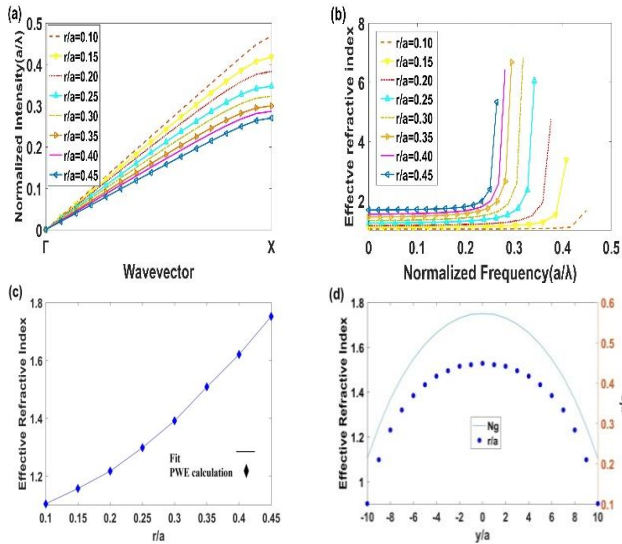

Fig. 2. (a) Dispersion diagram along Γ-X direction, (b) the effective refractive index as a function of normalized frequency and (c) the effective refractive index as a function of rod radius index (d) The parabolic effective refractive index curve and radius distribution curve for GRIN PC structure type I at fixed frequency 0.18

According to the ray theory the light rays bend towards the higher refractive index in the GRIN media [59]. As it is presumed from Fig. 2(d) and Fig. 3(d), the effective refractive index of both structures along the optical axis is larger than both sides and as a result, the incident wave converges towards the central region.

Both of the GRIN PC structures, type I and type II, are constructed from parabolic GRIN PC structure in which the effective refractive index comply with the following relation:

$$N^2(y) = N_0^2(1 - \alpha^2 y^2) \qquad (2)$$

Where N_0 would be the refractive index along the optical axis (x-direction) which is equal to 1.747 and 1.970 for structure type I and type II respectively and α stands as the gradient coefficient. Both of the GRIN PC structures are composed of 21 rows that make the y-direction in the range of [-10a, 10a]. The gradient coefficient of α regarding the GRIN PC structures, type I and type II, are 0.078 and 0.074 respectively. The required radius values for the refractive index distribution equation (2) are extracted from the fitting curve in Fig. 2(c) and 3(c),

concerning structure type I and type II respectively. The parabolic effective refractive index curve and radius distribution curve for these two particular structures are plotted in Fig. 2(d) and 3(d). Manipulation and controlling light propagation in a certain direction is based on the gradual changes of PCs structural parameter that cautiously modify the refractive index of the structure and result in changing the dispersion properties. GRIN PC structure is designed to curve the light propagation direction, while we have investigated beam propagation by studying the iso-frequency curves in wave vector space. Wave propagation direction is defined by the group velocity which is perpendicular to the iso-frequency curves. To achieve light bending, it is required to modify the direction of group velocity that travel through GRIN PC. Group velocity is position dependent within a GRIN PC structure.
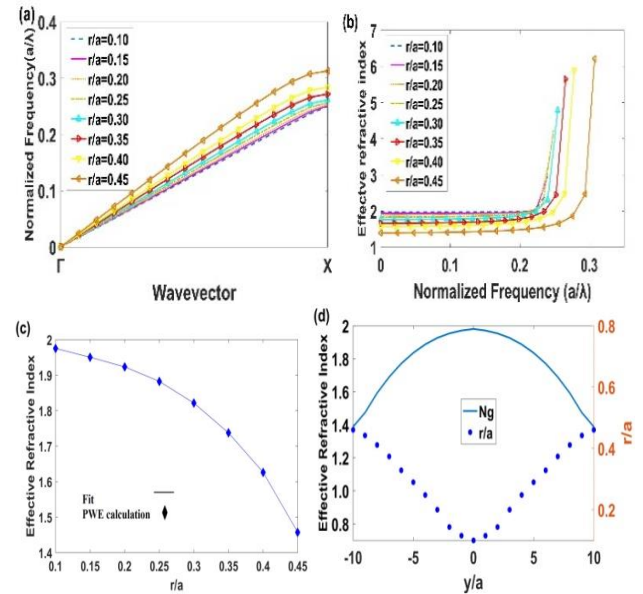

Fig. 3. (a) Dispersion diagram along Γ-X direction, (b) the effective refractive index as a function of normalized frequency and (c) the effective refractive index as a function of rod radius index (d) The parabolic effective refractive index curve and radius distribution curve for GRIN PC structure type II at fixed frequency 0.18

By utilizing this unique property of GRIN PC, it is possible to achieve continuous light bending. Although GRIN PCs are not strictly periodic, yet when the gradient of refractive index is small enough one can extract the optical properties from the normal PC. Arising from gradual changes in the filling factor of unit cells, group velocity seem to be position dependent and so the light propagation direction slowly changes as it travels through the structure. The iso-frequency curves of PCs that are made of dielectric rods with the radius equal to 0.30a, 0.35a, 0.40a and 0.45a are represented in Fig. 4. As it is indicated from Fig. 4, the iso-frequency curves are almost circular for the frequencies around 0.18 and the different

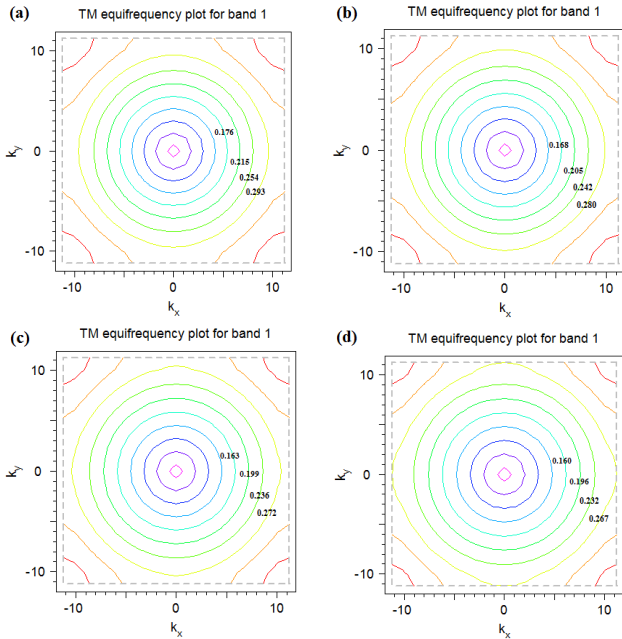values of r/a. Therefore, we can approximate the PC structure as an isotropic medium.

Fig. 4. Iso-frequency curves for PC structures with rod radius equal (a) 0.30a, (b) 0.35a, (c) 0.40a and (d) 0.45a

The main content can be classified as the following: in the first step, optical phenomena such as focusing, de-focusing, and collimation effect is investigated for the GRIN PC structure type I, while curving the incident wave fronts and creating focal point at the output of the structure has been monitored. In the second step, the different focusing characteristics of both structures have been enquired into and the obtained results have been compared.

3. Simulation results

In order to observe the focusing, collimation, and de-focusing effects, the GRIN structure is illuminated by a continuous wave with a Gaussian profile that is located at the left side of the structure. To perceive the field propagation throughout the structure, the FDTD method is carried out and the computational domain is surrounded by the Perfectly Matched Layer (PML). Focusing and de-focusing cases are displayed in Fig. 5(a) and 5(b).
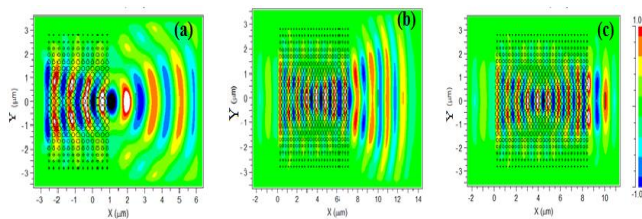

Fig. 5. Focusing, de-focusing and collimation behaviours of special cases of the proposed GRIN PC type I operating at a fixed frequency of a/λ=0.18 are presented at (a), (b) and (c), respectively

In the focusing case, we have a real focal point at the output of the structure while the wave fronts converge toward it. Regarding the de-focusing case, we have a virtual focal point inside the structure and the wave fronts start to diverge as they exit the structure. In the case of collimation effect, the wave fronts enter the structure and converge toward the virtual focal point; then, they diverge and exit the structure. When the beam gets out of the structure, wave fronts seem to be flat and collimated beam can be observed as it is demonstrated in Fig. 5(c).

As the second step, the dependency of focal point on different structural lengths is investigated. The focusing behavior of GRIN PC structure type I is analyzed with respect to the number of columns. The number of these particular columns is increased and the input wave revolution is examined. Fig. 6 presents a collection of output field patterns for various lengths of GRIN PC structure, which were considered to be {2a, 3a, 4a, 5a, 6a, 7a} at the normalized frequency of a/λ=0.18. Fig. 6 shows the spatial field distribution in which the focal point locality is specified by the dotted line. The objective is to compare the structure output distance from the focal points of the ones with different lengths. The structure is illuminated through a continuous wave with a Gaussian profile, in which the source is located at the left side of the GRIN PC structure. When it is only two columns, the GRIN PC displays focusing behavior and the structure effects the wave fronts by bending them slightly.
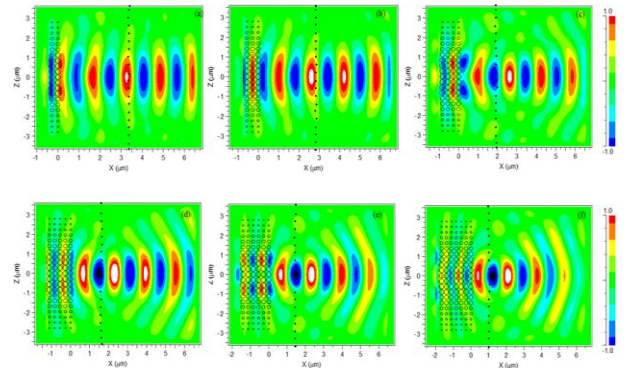

Fig. 6. The field distribution of the focusing effect for different lengths of structure type I, the length is equal to 2a, 3a, 4a, 5a, 6a, and 7a in (a), (b), (c), (d), (e), and (f), respectively

As shown in Fig. 6(b), when the number of columns is increased to 3, the focusing effect seem to be more apparent and a real focal point is created. As it is illustrated in Fig. 6(a) to 6(f), by increasing the length of GRIN PC structure up to 7a, the focal point gets closer to the ending face of structure. Although in Fig. 6(b) and 6(c), the structure length is equaled to 3a and 4a, yet there is not a significant difference between the positions of the focal point. The focusing effect is completely evident as the length of GRIN PC structure is increased from 5a to 7a, which is demonstrated in Fig. 6(d), 6(e), and 6(f) respectively. We can deduce that a very small GRIN PC is sufficient to focus a wide input beam on a narrow area. According to the results of Fig. 6(a)-(f), when the structure length is increased, the focal point moves closer to the

output surface. The mentioned results also show that the GRIN PC can perform as an optical element, capable of being used as an optical lens for focusing purposes.

In the following, we will compare the focusing characteristics of two GRIN PC structures, type I and type II. The structures are excited by a wide pulse at the frequency of a/λ=0.18. Fig. 7 shows the field propagation through the GRIN PC structures that contain different number of columns (N) as N escalates from 1 to 7 with step of 2. The focal point position is marked by dashed lines and the distance between the output surface of structures and the focal point position is defined as ΔF. According to the field patterns in Fig. 7, increasing the length of both structures leads to the following results: a) N changes from 1 to 7 with step-size of 2, b) the ΔF decreases gradually, and c) the focal point gets closer to the structure. Apart from these general results that has been extracted for both of the structures, yet there seem to be interesting differences among them. As it can be observed from Fig. 7 (a)-(d) that relate to the structure type I and Fig. 7(e)-(g) which is associated with structure type II, the way these two structures affect the input beam is a little bit different. When N is equaled to 1, the focal point is far from the output surface of structure type II; but regarding the other type, focal point seem to be closer to the structure. By increasing the number of columns at the same time, the focal point position changes and once the number reaches 7, it moves toward the structure.

On the other hand, as it is comprehended from Fig. 7, structure type II contains the broader range of focal point locality while more enhanced output beam is observed as well. In order to provide precise analyses about the focusing behavior of the considered GRIN PC configurations, we have studied the intensity profiles at the focal points of field distributions. The intensity profiles of field propagation, at a fixed frequency of a/λ=0.18 throughout the different lengths of the mentioned structures, have been plotted in Fig. 8 as N= {1, 3, 5, 7}.
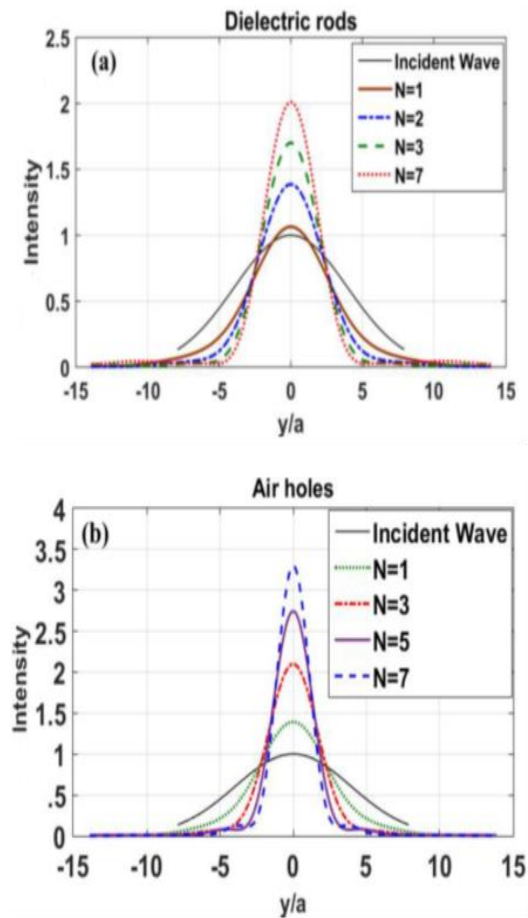
Fig. 8. Intensity profiles for N= {1, 3, 5, 7} at the focal point of the GRIN PC structures (a) type I and (b) type II

In the next step, we supplied a way to compare the focusing behavior of both structures. In order to study the focusing properties of the GRIN PC structures further, two peculiarities have been investigated that is mentioned in the following: a) the Full Width at Half Maximum (FWHM) and b) the distance between the structure and focal point position (ΔF). The FWHM is calculated from the field intensity at the focal point, while ΔF values are extracted from the field propagation throughout the GRIN PC structures. Results are shown in Table 1 and Table 2 concerning the structures type I and type II, respectively.
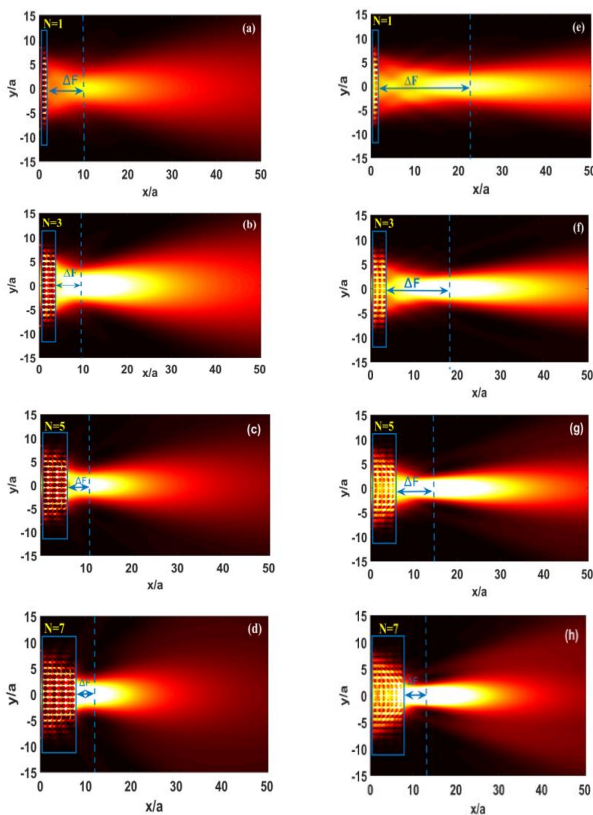

Fig. 7. The field propagation through the GRIN PC structures having 1, 3, 5 and 7 columns, for the structures type I and type II in (a)-(d) and (e)-(h), respectively

Table 1. FWHM and ΔF values for different structural length of structure type I

N	ΔF(a)	FWHM(a)	ΔF(λ)	FWHM(λ)
1	9.56a	6.75a	1.72 λ	1.22 λ
2	8.21a	6.36a	1.49 λ	1.14 λ
3	7.5a	6.03a	1.35 λ	1.09 λ
4	6.5a	6.03a	1.17 λ	1.09 λ
5	5.5a	5.75a	0.99 λ	1.04 λ
6	4.4a	5.6a	0.79 λ	1.01 λ
7	3.21a	5.53a	0.58 λ	0.99 λ
8	2.5a	5.35a	0.45 λ	0.98 λ
9	1.93a	5.46a	0.35 λ	0.96 λ
10	1.29a	5.25a	0.23 λ	0.96 λ

Table 2. FWHM and ΔF values for different structural length of structure type II

N	ΔF(a)	FWHM(a)	ΔF(λ)	FWHM(λ)
1	19.9a	6.48a	3.58λ	1.17 λ
2	15.3a	5.9a	2.75 λ	1.06 λ
3	12.9a	5.36a	2.32 λ	0.96λ
4	9.8a	4.85a	1.76 λ	0.87 λ
5	8.1a	4.48a	1.45 λ	0.80 λ
6	6.0a	4.17a	1.08 λ	0.75 λ
7	4.2a	3.92a	0.75 λ	0.70 λ
8	2.9a	3.76a	0.53 λ	0.67 λ
9	1.9a	3.63a	0.35 λ	0.65 λ
10	1.28a	3.55a	0.23 λ	0.64 λ

FWHM and ΔF values are presented in terms of the lattice constant (a) and wavelength (λ). Starting from N=1, the focal point is located at the distance of 9.56a and 19.9a from both of the structures, respectively. By increasing the number of columns N, ΔF decreases until it reaches 1.29a and 1.28a as N=10, in type I and type II, respectively. Consequently, by escalating N from 1 to 10, ΔF moved closer to the structures, while it varied from 9.56a to 1.29a for structure type I and 19.9a to 1.28a for structure type II. When the initial values of ΔF in terms of λ is compared, it can be deduced that the regarding values are different as 1.72λ versus 3.58λ, yet the last values reach 0.23λ equally. The second feature that brings more information about the focusing properties of the mentioned structures is FWHM value. The pattern of changing FWHM with respect to the increasing number of columns is different for two configurations. As N increases from 1 to 10, FWHM decreases from 6.75a to 5.25a for structure type I and decreases from 6.48a to 3.55a for structure type II. The FWHM results in term of wavelength (λ) unit in a similar manner that has been followed by both of the structures, would be 1.215λ to 0.94λ and 1.17λ to 0.64λ respectively. As it has been previously mentioned and can be clearly observed in Table 1, even one column is enough to perceive the focusing effects of the designed GRIN PCs. The structure with N=1 can change the spot size and compress the incident wave, which indicates that the designed GRIN PCs work very well similarly to a lens. In order to have more evident comparisons between the achieved results for the two mentioned structures, the FWHM values and the maximum values of intensity at focal point as a function of columns number have been plotted. Fig. 9 has demonstrated the results for both structures.
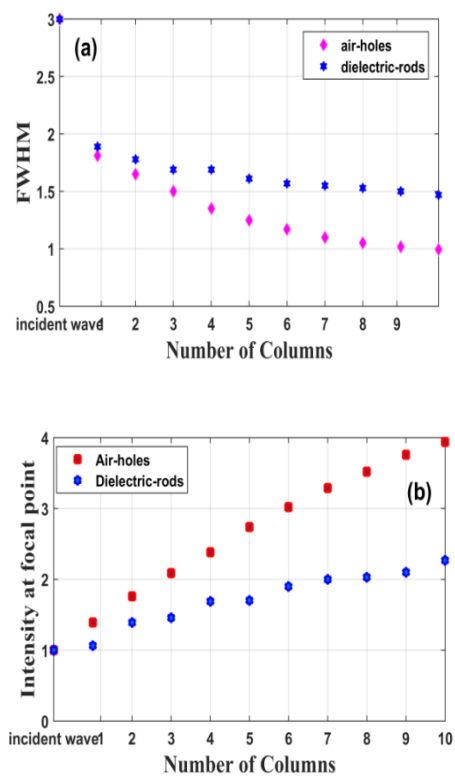

Fig. 9. (a) The FWHM values, (b) the maximum values of intensity at focal point as a function of columns number for both structures

As it is evident from Fig. 9(a), structure type II affects the incident wave more and reduces the FWHM values noticeably. In contrast, structure type I has a slower speed of changing the FWHM values as a function of the columns number. The achieved maximum values of normalized intensity for the structure type II has reached higher values in comparison to structure type I. Although structure type I can remarkably effect the input beam and focus it, yet structure type II shows better focusing features.

4. Conclusion

In this study, we derived various properties that were related to the focusing effects of designed GRIN PC structures. Different optical phenomena such as focusing, de-focusing, and collimation effects have been observed through the structure type I, while, several focusing characteristics were extracted from the structure type II. In addition, the obtained results were compared to the features that have been discovered by the structure type I. The employed computational approaches were two methods as the following: a) Plane Wave Expansion (PWE) procedure that is used to derive the suitable frequency which in turn is applied to legitimately show the focusing effect, and b) Finite-Difference Time-Domain (FDTD) method that is utilized to calculate the field distribution within the GRIN PC structures. According to the performed analysis and the previously obtained results, it can be suggested that the structure clearly affects the propagation direction of waves and we have also proved that fewer number of columns are enough to produce a focal point with strong focusing power. The electromagnetic field propagation through GRIN PC structures has been monitored and strong focusing behavior has been observed. The simulations indicate that the designed GRIN PC focuses the incident wave to a narrow area. Furthermore even one column is enough to observe focusing effect. As a result, the designed GRIN PC structures showed strong focusing behavior. In fact, the designed GRIN PC works very well as a lens with adjustable focusing features that seem to be quiet suitable for practical implements.

References

[1] E. Yablonovitch, Phys. Rev. Lett. **58**(20), 2059 (1987).

[2] S. John, Phys. Rev. Lett. **58**(23), 2486 (1987).

[3] H. Kosaka, T. Kawashima, A. Tomita, M. Notomi, T. Tamamura, T. Sato, et al., Phys. Rev. B **58**(16), R10096 (1998).

[4] J. Amet, F. Baida, G. Burr, M. P. Bernal, Photonic. Nanostruct. **6**(1), 47 (2008).

[5] H. Kosaka, T. Kawashima, A. Tomita, M. Notomi, T. Tamamura, T. Sato, et al., Appl. Phys. Lett. **74**(9), 1212- 4 (1999).

[6] T. T. Kim, S. G. Lee, H. Y. Park, J. E. Kim, C. S. Kee, Opt. Express **18**(6), 5384-9 (2010).

[7] Y. Zhang, Y. Zhang, B. Li, Opt. Express **15**(15) 9287- 92 (2007).

[8] D. Chigrin, S. Enoch, C. S. Torres, G. Tayeb, Opt. Express **11**(10) 1203-11 (2003).

[9] D. W. Prather, S. Shi, D. M. Pustai, C. Chen, S. Venkataraman, A. Sharkawy, et al., Opt. Lett. **29**(1), 50-2 (2004).

[10] T. Baba, D. Mori, Journal of Physics D: Applied Physics **40**(9), 2659 (2007).

[11] C. Luo, S. G. Johnson, J. Joannopoulos, J. Pendry, Phys. Rev. B. **65**(20), 201104 (2002).

[12] W. D. Zhou, J. Sabarinathan, P. Bhattacharya, B. Kochman, E. Berg, P. C. Yu, S. Pang, IEEE J. Quant. Electron. **37**(9), 1153 (2001).

[13] W. Zhou, Z. Qiang, L. Chen, J. Phys. D Appl. Phys. **40**(9), 2615 (2007).

[14] L. Sanchis, M. J. Cryan, J. Pozo, I. J. Craddock, J. G. Rarity, Phys. Rev. B **76**(4), 045118 (2007).

[15] W. Jia, J. Deng, A. M. Sahadevan, H. Wu, L. Jiang, X. Li, A. J. Danner, Appl. Phys. Lett. **98**(24), 241102 (2011).

[16] H. Kurt, D. S. Citrin, IEEE J. Quant. Electron. **43**(1), 78 (2007).

[17] M. Lončar, J. Vučković, A. Scherer, J. Opt. Soc. Am. B **18**(9), 1362 (2001).

[18] Y. Watanabe, N. Ikeda, Y. Takata, Y. Kitagawa, N. Ozaki, Y. Sugimoto, K. Asakawa, J. Phys. D Appl. Phys. **41**(17), 175109 (2008).

[19] J. D. Joannopoulos, R. D. Meade, J. N. Winn, Photonic Crystals: Molding the Flow of Light, 2nd ed., Princeton University Press, Princeton, 2008.

[20] M. H. Shih, Y. C. Yang, Y. C. Liu, Z. C. Chang, K. S. Hsu, M. C. Wu, J. Phys. D Appl. Phys. **42**(10), 105113 (2009).

[21] Y. R. Zhen, L. M. Li, J. Phys. D Appl. Phys. **38**(18), 3391 (2005).

[22] T. Yu, H. Zhou, Z. Gong, J. Yang, X. Jiang, M. Wang, J. Phys. D Appl. Phys. **41**(9), 095101 (2008).

[23] H. Kurt, D. S. Citrin, Appl. Phys. Lett. **87**(4), 041108 (2005).

[24] Y. Fink, J. N. Winn, S. Fan, C. Chen, J. Michel, J. D. Joannopoulos, E. L. Thomas, Science **282**(5394) 1679 (1998).

[25] S. Noda, A. Chutinan, M. Imada, Nature **407**(608), 6804 (2000).

[26] H. Kurt, D. S. Citrin, Opt. Express **15**(3), 1240 (2007).

[27] H. Kurt, E. Colak, O. Cakmak, H. Caglayan, E. Ozbay, Appl. Phys. Lett. **93**(17), 171108 (2008).

[28] H. W. Wang, L. W. Chen, J. Appl. Phys. **109**(10), 103104 (2011).

[29] E. Akmansoy, E. Centeno, K. Vynck, D. Cassagne, J. M. Lourtioz, Appl. Phys. Lett. **92**(13), 133501 (2008).

[30] A. O. Cakmak, E. Colak, H. Caglayan, H. Kurt, E. Ozbay, J. Appl. Phys. **105**(10), 103708 (2009).

[31] D. Yilmaz, I. H. Giden, M. Turduev, H. Kurt, IEEE J. Quant. Electron. **49**(5), 477 (2013).

[32] X. Le Roux, C. Caer, D. Marris-Morini, N. Izard, L. Vivien, E. Cassan, IEEE Photon. Tech. Lett. **23**(15), 1094 (2011).

[33] H. Kurt, B. B. Oner, M. Turduev, I. H. Giden, Opt. Express **20**(20), 22018 (2012).

[34] B. B. Oner, M. Turduev, I. H. Giden, H. Kurt, Opt. Lett. **38**(2), 220 (2013).

[35] E. Centeno, D. Cassagne, Opt. Lett. **30**(17), 2278 (2005).

[36] E. Centeno, D. Cassagne, J. P. Albert, Phys. Rev. B. **73**(23), 235119 (2006).

[37] H. Kurt, D. S. Citrin, Opt. Express **15**(3), 1240 (2007).

[38] H. Kurt, E. Colak, O. Cakmak, H. Caglayan, E. Ozbay, Appl. Phys. Lett. **93**(17), 171108 (2008).

[39] E. Akmansoy, E. Centeno, K. Vynck, D. Cassagne, J. M. Lourtioz, Appl. Phys. Lett. **92**(13), 133501 (2008).

[40] M. Lu, B. K. Juluri, S. C. S. Lin, B. Kiraly, T. Gao, T. J. Huang, J. Appl. Phys. **108**(10), 103505 (2010).

[41] N. Yogesh, V. Subramanian, Electromagn. Res. **129**, 51 (2012).

[42] B. B. Oner, M. Turduev, H. Kurt, Opt. Lett. **38**(10), 1688 (2013).

[43] M. Turduev, I. H. Giden, H. Kurt, Opt. Commun. **339**, 22 (2015).

[44] F. Gaufillet, É. Akmansoy, Opt. Mater. **47**, 555 (2015).

[45] A. Gharaati, N. Miri, Ukr. J. Phys. Opt. **18**(2), 109 (2017).

[46] I. H. Giden, B. Rezaei, H. Kurt, J. Opt. Soc. Am. B. **32**(10), 2153 (2015).

[47] B. Rezaei, I. H. Giden, H. Kurt, Opt. Commun. **382**, 28 (2017).

[48] E. Miyai, K. Sakai, T. Okano, W. Kunishi, D. Ohnishi, S. Noda, Nature. **441**, 946 (2006).

[49] Y. Z. Liu, S. Feng, J. Tian, C. Ren, H. H. Tao, Z. Y. Li, B. Y. Cheng, D. Z. Zhang, J. Appl. Phys. **102**(4), 043102 (2007).

[50] K. Ren, X. Ren, Chin. Sci. Bull. **57**(11), 1241 (2012).

[51] K. Ren, X. Ren, Appl. Opt. **50**(15), 2152 (2011).

[52] A. Gharaati, S. H. Zahraei, Advances in Optical Technologies **2014**, (2014).

[53] U. G. Yasa, M. Turduev, I. H. Giden, H. Kurt, J. Lightwave Tech. **35**(9), 1677 (2017).

[54] B. Tellioğlu, E. Bor, M. Turduev, H. Kurt. In Transparent Optical Networks (ICTON), 2016 18th International Conference on (pp. 1-4). IEEE.

[55] I. H. Giden, N. Eti, B. Rezaei, H. Kurt, IEEE J. Quantum. Elect. **52**(10), 1 (2016).

[56] N. Miri, A. Gharaati, Journal of Optoelectronical Nano Structures **2**(2), 55 (2017).

[57] A. Taflove, S. C. Hagness, 2nd Ed Artech House Publishers, 2005.

[58] A. Igor Sukhoivanov, Igor V. Guryev, Springer Photonic Crystals **152**, 2009.

[59] C. Gomez-Reino, M. V. Perez, C. Bao, Springer Science & Business Media, 2012.

*Corresponding author: agharaati@pnu.ac.ir